Journal of Engineering and Sustainable Development
http://jeasd.uomustansiriyah.edu.iq
https://doi.org/10.31272/jeasd.24.6.4

JEASD

Vol. 24 No. 06, November 2020
ISSN 2520-0917

DESIGN AND PERFORMANCE ANALYSIS OF ORTHOGONAL MULTI-LEVEL CODE-SHIFTED DIFFERENTIAL CHAOS SHIFT KEYING COMMUNICATION SYSTEM

***Hayder F. Fahad[1]** **Fadhil S. Hassan[2]**

1) M.Sc, Student, Electrical Engineering Department, Mustansiriyah University, Baghdad, Iraq
2) Assistant Prof. Dr., Electrical Engineering Department, Mustansiriyah University, Baghdad, Iraq

Received 13/1/2020 ***Accepted in revised form 26/4/2020*** ***Published 1/11/2020***

Abstract: Based on Orthogonal Chaotic Vector Shift Keying (OCVSK) system and Multilevel Code-Shifted Differential Chaos Shift Keying (MCS-DCSK) system, a new Multilevel Code-Shifted Differential Chaos Shift Keying (OMCS-DCSK) modulation system is proposed and designed in this paper. New orthogonal chaotic signal sets are generated using Gram-Schmidt algorithm and Walsh code function then these signals are used for bearing information bits to achieve higher data rate and better bandwidth efficiency compared with the conventional DCSK communication system. The bit error rate (BER) analysis of the OMCS-DCSK system over additive white Gaussian noise (AWGN) and multipath Rayleigh fading channel is derived and compared with the simulation results. Also, the spectral and complexity analysis of the system are presented and compared with the conventional DCSK systems. The results show that the proposed system outperforms OCVSK and MCS-DCSK in BER performance and spectral efficiency

Keywords: *Multilevel code-shifted differential chaos shift-keying, orthogonal chaotic vectors, Gram-Schmidt algorithm, Walsh function, high data rate.*

1. Introduction

Throughout the previous time, applying chaotic signals have been devoted much hard work in digital communications as a spread spectrum [1]-[16]. On a fundamental level, the impacts of digital modulation and spectrum spreading can be accomplished by mapping the information into several properties of the wideband chaotic waveforms. Unlike the conventional spread spectrum system, chaotic modulation utilizes aperiodic chaotic signals as carriers described by the very sensitivity to initial condition values, minimum cost generation, and good correlation properties. As a consequence, chaotic modulations demonstrate lots of appealing features that are good communication security, unpretentious transmitter and receiver circuits, solid immunity to self-interference, interception with lower probability, and good bit-error-rate (BER) performances under multipath fading channel [1], [2].

Chaos based digital communication system can be classified into two classes: coherent and non-coherent schemes. In coherent schemes like chaos shift keying (CSK) system, the synchronization of the carrier's synchronization between transmitter and receiver must be achieved, which is still a challenging task today [2]. Therefore, it is not possible to practice coherent schemes. In other words, the non-coherent scheme like differential chaos shift keying (DCSK) sends the reference chaotic signal with information signal in different time

**Corresponding Author*: haider.fadhil.fahad@gmail.com

slots. Therefore, the need for chaotic synchronization is ignored [3].

In the DCSK system, the transmitted signal is divided into two equal lengths of time slots containing one reference sequence in the first time slot and reference signal multiplied by either -1 or 1 which represents the information bits of 0 and 1 respectively in the second time slot. DCSK system in this simple form has a weakness in terms of information security because the reference itself is transmitted with the modulated signal and has a lower data rate compared with CSK for the same reason where half of the transmitted signal is reference signal [4]. In order to improve the data rate or enhance the energy efficiency, many enhanced algorithms are applied for the DCSK system, such as Hilbert transform filter that is used in Quadrature chaos shift keying (QCSK) to double data rate [5]. The Gram-Schmidt process that is used in orthogonal chaotic vector shift keying (OCVSK) instead of Hilbert conversion to allow the information sequence carries *M* bits instead of one in DCSK or two in QCSK in the same time slot, where *M* is the number of reference orthogonal chaotic signals that is generated by Gram-Schmidt algorithm [6]. Walsh code function that is used in *M*-ary DCSK to improve the data rate and increase the efficiency of the bandwidth relatively [7]. Also, Walsh code is used in code shifted-DCSK (CS-DCSK) which can send both the reference and information signals at the same time slot and increase the data rate with no delay line at the receiver [8]. Other versions of *M*-ary DCSK and CS-DCSK is Multilevel Code-Shifted Differential Chaos Shift Keying (MCS-DCSK) which improved the bandwidth efficiency and reduces the complexity of the previous proposal and the ability to send (*M*-2) to the Walsh code utilizes (*M*) [9] and Orthogonal Multilevel DCSK (OM-DCSK) in which the original reference part is included with the information directly and the other part enters the Hilbert conversion [10]. Further approaches to enhance the data rate by reducing the impact of reference sequences are those proposed in phase-separated DCSK (PS-DCSK) [11], improved DCSK (I-DCSK) [12], short reference DCSK (SR-DCSK) [13] and initial condition-index chaos shift keying [14].

In other techniques to improve the data rate, energy efficiency and RF delay line are combined multicarrier techniques with DCSK [15-19]. In [15] and [16] DCSK system is designed with multicarrier modulation to produce multicarrier DCSK (MC-DCSK) system, in which the chaotic signals are sent in multicarrier form instead of single carrier modulation system. In [17], orthogonal frequency division multiplexing (OFDM) based DCSK (OFDM-DCSK) is proposed in which the OFDM system is used to improve DCSK system. Also, OFDM can be used with other versions of DCSK like short reference QCSK (SR-QCSK) (OFDM-SRQCSK) [18], OCVSK (OFDM-OCVSK) [19].

In recent years, there are a growing interest in index modulation (IM) techniques, which are viewed as creative approaches to pass on information compared to conventional communication systems with the engaging advantages to improve spectral and energy efficiency and data rate [20]. In [21] permutation index DCSK (PI-DCSK) is proposed with the goal of increasing energy efficiency and information rate. Code index modulation (CIM) techniques can be combined with DCSK system in efficient way as in [22], [23] and [24]. Also, CIM is combined with CS-DCSK as in [25], and with OM-DCSK as in [26].

In this paper, a new design of a high data rate communication system is presented which combines orthogonal chaotic vectors and the multilevel code shifted DCSK and named orthogonal multilevel code shifted DCSK (OMCS-DCSK) modulation. The new system differs from orthogonal multilevel DCSK (OM-DCSK) [1،] in which the Hilbert transform is replaced with Gram-Schmidt algorithm to produce new versions of orthogonal sets. These new orthogonal basis signals are used to carry the information in the same time slot and increased the effectiveness of the information rate and the energy of the system. To prove the effectiveness of the suggested OMCS-DCSK

system, the analytic BER is derived over AWGN and multipath Rayleigh fading channels and compared with the simulation results with different system parameters. Also, the information rate and energy efficiency are considered and compared with orthogonal chaotic vector shift keying (OCVSK)[٦] and multilevel code shifted DCSK (MCS-DCSK)[9] communication systems. Finally, the BER performance and complexity analysis are compared between the suggested system and other conventional DCSK-based systems.

The rest of the paper is organized as follows: In section II, Gram Schmidt, Walsh code and the structures of transmitter and receiver of the OMCS-DCSK are described. In section III, the derivation of analytic OMCS-DCSK BER and the complexity are presented. The simulation results in AWGN and multipath fading channels are described in section IV. Finally, the conclusions are presented in section V.

2. Orthogonal Multi-Level Code Shifted Dcsk System

In this section, the design of orthonormal basis function sets using Gram-Schmidt and Walsh code function and the transceiver architecture of the OMCS-DCSK system are presented.

2.1. Repeated Orthogonal Chaotic Generator (ROCG)

Fig. 1 shows repeated orthogonal chaotic generator (ROCG). Firstly the source of *N* non-orthogonal chaotic signals, $x_0^{(n)}, x_1^{(n)}, \dots\dots, x_{N-1}^{(n)}$ are generated either from different chaotic systems or from a chaotic system with different initial values, where $0 \leq n < R$ and R is the spread factor length. According to [19] these chaotic vectors are linearly independent for large value of R, where $R \geq N$. The chaotic signal can be generated by Chebyshev second-order equation Multiprocessor Function (CPF) with unity variance and zero mean as [13]

$$x_{k+1} = 1 - 2x_k^2 \quad (1)$$

The resulting chaotic signals are entered into the Gram-Schmidt algorithm to obtain N orthogonal chaotic vectors $e_0^{(n)}, e_2^{(n)}, \dots, e_{N-1}^{(n)}$ using the following process [19]:

$$e_j^{(n)} = \begin{cases} x_0^{(n)} & for\ j = 0 \\ x_j^{(n)} - \sum_{i=1}^{j-1} \frac{\left\langle x_j^{(n)}, e_i^{(n)} \right\rangle}{\left\langle e_i^{(n)}, e_i^{(n)} \right\rangle} e_i^{(n)}, & for\ j = 1, \dots, N-1 \end{cases} \quad (2)$$

where $\left\langle x_j^{(n)}, e_i^{(n)} \right\rangle$ is the inner product of the sequences $x_j^{(n)}$ and $u_i^{(n)}$ that is given by:

$$\left\langle x_j^{(n)}, e_i^{(n)} \right\rangle = \sum_{n=0}^{R-1} x_{j,n} e_{i,n} \quad (3)$$

and $x_{j,n}$ is the *n*-th sample of the *j*-th chaotic vector and $e_{i,n}$ is the *n*-th sample of the *i*-th vector $e_i^{(n)}$. To have unit energy, the orthogonal signals in (1) are normalized according to:

$$x_{gj}^{(n)} = \frac{e_j^{(n)}}{\sqrt{\left\langle e_j^{(n)}, e_j^{(n)} \right\rangle}}, for\ j = 0, \dots, N-1 \quad (4)$$

where $x_{gj}^{(n)}$ is the *j*-th orthonormal chaotic reference sequence, $0 \leq n < R$.

In order to produce chaotic basis signals from each *j*-th reference signal, $Xgj = [x_{gj}^{(0)}\ x_{gj}^{(1)}\ \dots\dots x_{gj}^{(R-1)}]$, $X_{gj} \in \mathbb{R}_{N \times R}$, $j = 0,1,..,N-1$, repeated orthogonal chaotic generator (ROCG) is used for each *j*-th signal as shown in Fig. 1. Each symbol duration *T* is then divided into *M* time slots, where $M=2^{z-1}$ and *z* is an integer value. For *j*-th group, ROCG directly produces $x_g^{(n)}(j,i), 0 \leq n < R$, generated by the *j*-th orthonormal chaotic signal , $x_{gj}^{(n)}$. This signal is then delayed and duplicated for (*M*-1) times to generate the sequences, $X_g(j,i) \in \mathbb{R}_{N \times M \times R}$, $0 \leq j < N$, $0 \leq i < M$. Then, from the duplication process and Walsh code function *M* orthonormal chaotic basis signals can be generated for each *j*-th group as seen in the next subsection. Therefore, there are *MN* orthonormal chaotic signals can be generated in each symbol duration.

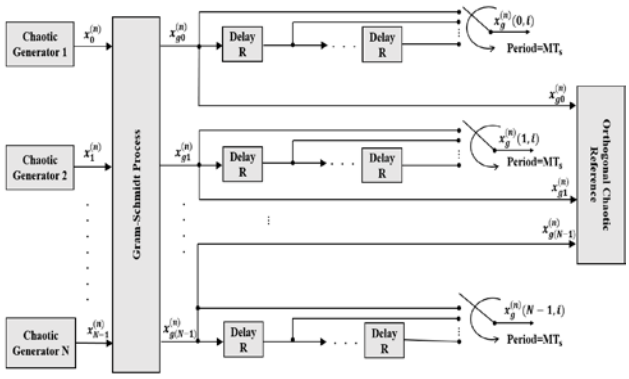

Figure 1. Structure of ROCG.

2.2. *OMCS-DCSK Scheme*

The distinguishing feature of the proposed OMCS-DCSK system is that it combines the Gram-Schmidt algorithm and the Walsh code. This technique is proposed to increase spectral efficiency and enhance the noise performance of the system. The main idea of OMCS-DCSK is designing orthonormal basis sets in efficient way comparing with OCVSK and MCS-DCSK and use them to carry MN bits at the same time slot instead of *N* bits and *M* bits as OCVSK and MCS-DCSK system respectively. In this section, the transmitter and receiver schemes of OMCS-DCSK system are presented and demonstrated in details.

2.2.1. Transmitter

Fig. 2 shows the block diagram of OMCS-DCSK transmitter. In the first, the serial bits b_{m} of m-th symbol duration are converted into the bipolar symbol, a_m according to $a_m = 2b_m - 1$, where $a_m \in \{+1, -1\}$. Then converted into *MN* parallel symbols, $a_{m,i+jM}$, *j*=0,...*N-1* and *i*=0,..,*M*-1. These *MN* symbols are then carried by *MN* orthonormal reference signals at the same time slot. For each *j*-th group, *M* orthonormal chaotic signals of length *MR* samples are generated using ROCG process and Walsh function according to

$$x_b^{(q)}(\mathrm{j},\mathrm{i}) = \sum_{k=0}^{M-1} W_{ik} x_{gj}^{(n)} rect(n-kR) \quad , \quad 0 \le i < \mathrm{M} \quad 0 \le q < MR \quad 0 \le j < \mathrm{N}' \quad 0 \le n < R \tag{5}$$

where W_{ik} is the *i*-th row and *k*-th column of Walsh code that is generated using Hadamard matrix as

$$W_{2^z} = \begin{bmatrix} W_{2^{z-1}} & W_{2^{z-1}} \\ W_{2^{z-1}} & -W_{2^{z-1}} \end{bmatrix} for\ z = 1,2,.. \tag{6}$$

and W_{2^0}=[1]. Also, $rect(n-kR)$is a discrete rectangular function that is expressed as

$$rect(n-kR) = \begin{cases} 1 & kR \le n < (k+1)R \\ 0 & otherwise \end{cases} \tag{7}$$

There are *MN* orthonormal chaotic signals, $X_b(\mathrm{j},\mathrm{i}) \in \mathbb{R}_{N\times N\times MR}$. This basis is then used to carry *MN* data bits at the same time slot. The structure of *j*-th orthonormal chaotic signals is shown in Fig.3. It is easily proved that any two orthonormal chaotic signals are orthogonal accordingly

$$\sum_{q=0}^{MR-1} x_b^{(q)}(j,i) x_b^{(q)}(u,v) = 0, \quad (j,i) \ne (u,v), \begin{matrix} j,u = 0,1,..,N-1 \\ i,v = 0,1,..,M-1 \end{matrix} \tag{8}$$

For OMCS-DCSK system, the baseband discrete transmitted signal can be expressed as

$$S_m(n) = \begin{cases} x_{g0}^{(n)} & for(0 \le n < R) \\ x_{g2}^{n} & for(R \le n < 2R) \\ \vdots & \\ x_{g(N-1)}^{(n)} & for\big((N-1)R \le n < NR\big) \\ \frac{1}{\sqrt{MN}} \sum_{j=0}^{N-1} \sum_{i=0}^{M-1} a_{m,(i+jM)}\, x_b^{(n)}(\mathrm{j},\mathrm{i}) & for(\ NR \le\ n < (N+M)R) \end{cases} \tag{9}$$

The first *N* time slots contain the chaotic reference signals, $[x_{g1}^{(k)}\ x_{g2}^{(k)}\ \ldots..x_{gN}^{(k)}]$ with length *NR* samples. The last time slot contains the data bearing signal that is expressed as

$$y_d(n+kR) = \frac{1}{\sqrt{MN}} \sum_{j=0}^{N-1} \sum_{i=0}^{M-1} a_{m,i+jM} W_{ik}\, x_r(j, n+kR) \qquad 0 \le n < R \ , \ 0 \le k < M \tag{10}$$

where $x_r(j,n+kR)=[x_{g0}^{(n)}\ x_{g1}^{(n)} \dots x_{gN-1}^{(n)}]$ is the j-th duplicated orthonormal chaotic signals, $x_r \in \mathbb{R}_{N\times MR}$.

The frame of the transmitted signal is shown in Fig. 4. There are NR samples for reference chaotic signal with N time slots and MR samples for information bearing signal with one time slot. The total time slot is (M+1) and the total length is (N+M)R samples. The corresponding frame duration becomes $T_{OMCS\text{-}DCSK} = (M+N)RT_c$, where T_c is the chip time. Also, the energy of the transmitted signal can be computed by $E_b = \frac{(M+N)R}{MN} E\left[\left(x_{gj}^n\right)^2\right]$, where E[.] is the expected value operator.

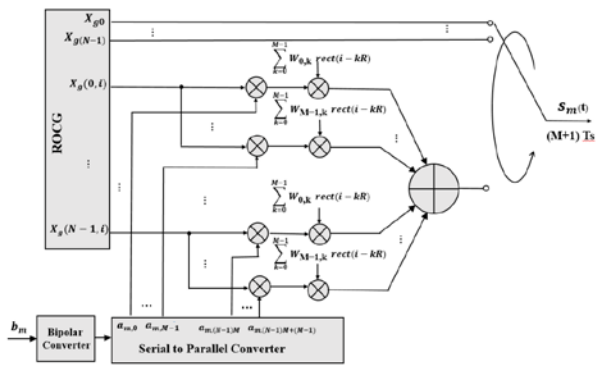

Figure2. Block diagram of OMCS-DCSK transmitter.

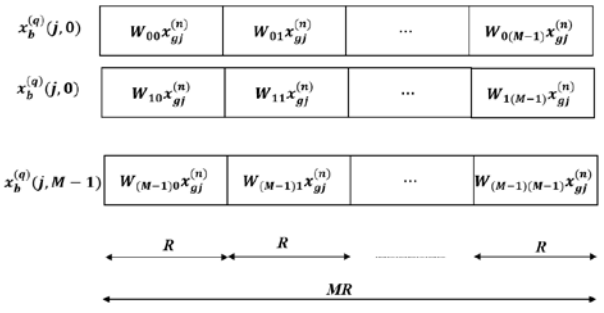

Figure3. The structure of j-th orthonormal chaotic signals.

$$r_{b(n+kR)}(\mathrm{j},\mathrm{i}) = \sum_{k=0}^{M-1} W_{ik}\, x_{r(j,n+kR)} + \xi_{(j,n+kR)} \tag{14}$$

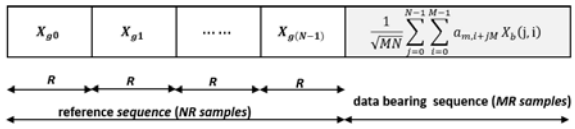

Figure4. OMCS-DCSK frame.

2.2.2. Receiver

The block diagrams of the OMCS-DCSK receiver is shown in Fig.5. The m-th symbol duration transmitted signal, $S_m(n)$ is corrupted with AWGN channel, $\xi(n)$ with zero mean and two sided power spectral density of $N_0/2$. The received signal of the m-th symbol duration, $r_m(n)$ is described by

$$r_m(n) = S_m(n) + \xi(n),\ 0 \le n < (M+N)R \tag{11}$$

To recover the transmitted bits, the reference chaotic signals and data bearing signal must be extracted from the received sequence. The j-th reference chaotic signal at the receiver can be expressed by

$$r_g^{(n)}(\mathrm{j}) = x_{gj}^{(n)} + \xi_{(\mathrm{n+jR})},$$

$$j = 0,..,N-1 \text{and } n = 0,1,..,R-1 \tag{12}$$

Each reference chaotic signal is duplicated M times using repeated orthogonal chaotic at the receive (ROCR) as shown in Fig. 6 to produce

$$y_r^{(n)}(\mathrm{j,i}) = r_g^{(n)}(\mathrm{j}), \quad i=0,..,M-1, \quad j=0,..,N-1. \tag{13}$$

The received basis signals are generated by multiplying the reference chaotic signal with the Walsh code according to

and the received data bearing signal can be expressed by

$$y_d(n+kR) = \frac{1}{\sqrt{MN}} \sum_{j=0}^{N-1} \sum_{i=0}^{M-1} a_{m,i+jM} W_{ik}\, x_{r(j,n+kR)} + \xi_{(n+MR+kR)} \quad 0 \le k < M, 0 \le n < R \qquad (15)$$

To recover the *v*-th transmitted bits in the *u*-th group, the received data bearing signal, $y_d(n+kR)$ is multiplied by the signal, $r_b^{(n+kR)}(u,v)$ and the energy value is calculated and compared to a zero threshold. The output of the *v*-th correlator in the *u*-th group is calculated as

$$Z_{u,v} = \sum_{k=0}^{M-1} \sum_{n=0}^{R-1} r_{b(n+kR)}(u,v)\, y_d(n+kR), \quad 0 \le u < N, 0 \le v < M \qquad (16)$$

The *u*-th recovered bit in the *v*-th group, $\hat{a}_{m,u+vM}$ is calculated from the decision value D_{u+vM} by comparing the correlator output, $Z_{u,v}$ with a zero threshold value. After that the parallel to serial converter is used to get the stream recovered bits.

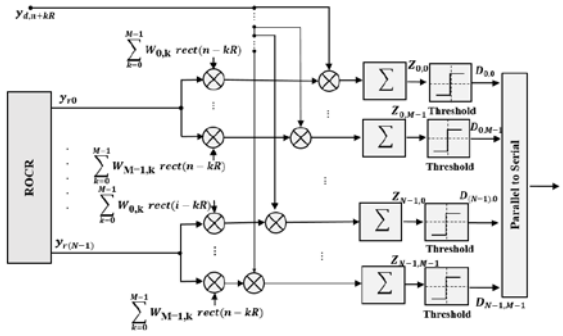

Figure 5. Block diagram of OMCS-DCSK receiver.

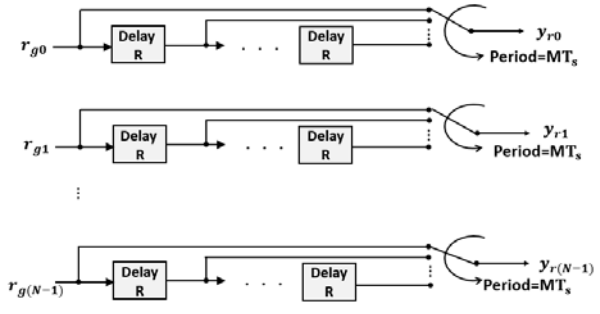

Figure 6. Structure of ROCR.

3. Performance Analysis

In this section, the analytical BER of OMCS-DCSK system is derived under multipath Rayleigh fading channel and AWGN. Also, the spectral and rate analysis of the proposed system are introduced.

3.1. Channel Model

The channel model of the Rayleigh multipath fading consists of *L* independent paths and equally distributed is shown in Fig. 7. This channel is widely utilized in spread spectrum wireless communication systems [16], [27]. The output signal of *L*-ray Rayleigh multipath fading channel for *m*-th symbol duration is expressed by

$$r_m(n) = \sum_{l=1}^{L} \alpha_l\, S_m(n-\tau_l) + \xi(n) \qquad (17)$$

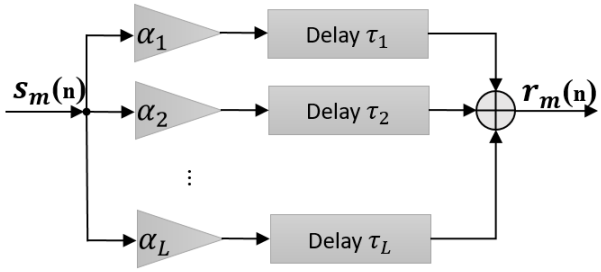

Figure 7. Multipath Rayleigh fading channel model.

where τ_l, α_l is the time delay and spread gain of the *l*-th path respectively. These *L* spread gains are independent and identically distributed (i.i.d.) random variables with Rayleigh probability density function (PDF) is given by [28]

$$f(\alpha|\sigma) = \frac{\alpha}{\sigma^2} \exp\left(\frac{\alpha^2}{2\sigma^2}\right) \qquad (18)$$

where σ > 0 is the scale parameter of the distribution which is the root mean square value of the received voltage sequence. The parameter, α_l is fixed during the entire symbol duration because the channel is assumed to be slowly fading.

3.2. *BER Analysis*

Assume that the maximum multipath delay τ_{max} is much smaller than the number of samples, $(N+M)R$ samples in one symbol duration, i.e., $0 < \tau_{max} \ll (N+M)R$ and the interference between each symbol is negligible because of the multipath time delay [19].

For simplicity the symbol *m* is ignored. To detect the first bit in the first group (j=0, i=0), the output of the correlator under multipath fading channel and AWGN is expressed as

---

$$Z_{0,0} = \sum_{k=0}^{M-1} W_{0,k} \sum_{n=0}^{R-1} \left(\sum_{l=1}^{L} \alpha_l \, x_{r(0,n+kR-\tau_l)} \, \xi_{(0,n+kR)} \right) \left(\frac{1}{\sqrt{MN}} \sum_{j=0}^{N-1} \sum_{i=0}^{M-1} \sum_{k=0}^{M-1} \sum_{n=0}^{R-1} \sum_{l=1}^{L} \alpha_l a_{i+jM} x_{r(j,n+kR-\tau_l)} W_{ik} + \xi_{(n+MR+kR)} \right) \quad (19)$$

Also,

$$Z_{0,0} = \sum_{k=0}^{M-1} W_{1,k} \sum_{n=0}^{R-1} \left\{ \frac{1}{\sqrt{MN}} \sum_{j=0}^{N-1} \sum_{i=0}^{M-1} \sum_{l=1}^{L} \alpha_l^2 \, W_{ik} a_{jM+i} x_{r(j,n+kR-\tau_l)} x_{r(0,n+kR-\tau_l)} + \left(\frac{1}{\sqrt{MN}} \sum_{j=0}^{N-1} \sum_{i=0}^{M-1} \sum_{l=1}^{L} \alpha_l \; a_{i+jM} \, x_{r(j,n+kR)-\tau_l} \; W_{ik} \, \xi_{(0,n+kR)} \right) + \sum_{l=1}^{L} \alpha_l \, x_{r(0,n+kR-\tau_l)} \; \xi_{(n+MR+kR)} + \xi_{(0,n+kR)} \, \xi_{(n+MR+kR)} \right\} \quad (20)$$

According to (8) and using the orthogonality between the reference chaotic signals, the following expression is valid

---

$$\sum_{i=0}^{R-1} x_{r(0,n+kR-\tau_l)} \, x_{r(j,n+kR-\tau_l)} \approx 0 \;, j \neq 0 \quad (21)$$

$$\sum_{i=0}^{R-1} x_{g0(n)} \, x_{g(j,n)} \approx 0 \qquad j \neq 0 \quad (22)$$

Substituting $a_{jM+i} = +1$, then (20) becomes

$$Z_{0,0} = \sum_{k=0}^{M-1} W_{1,k} \sum_{n=0}^{R-1} \left\{ \frac{1}{\sqrt{MN}} \sum_{l=1}^{L} \alpha_l^2 \, W_{ik} \, x_{r(0,n+kR-\tau_l)}^2 + \left(\frac{1}{\sqrt{MN}} \sum_{j=0}^{N-1} \sum_{i=0}^{M-1} \sum_{l=1}^{L} \alpha_l \; x_{r(j,n+kR)-\tau_l} \; W_{ik} \, \xi_{(0,n+kR)} \right) + \sum_{l=1}^{L} \alpha_l \, x_{r(0,n+kR-\tau_l)} \; \xi_{(n+MR+kR)} + \xi_{(0,n+kR)} \, \xi_{(n+MR+kR)} \right\} \quad (23)$$

The first term in (23) represents the desired energy signal while the remaining terms are the interference energy signals. The conditional expectation and the variance of $Z_{0,0}$ are calculated respectively as

$$E\left[Z_{0,0}\right] = \frac{1}{\sqrt{MN}} \, MR \, \sum_{l=1}^{L} \alpha_l^2 \; E\left[(x_{g0}^n)^2 \right] \quad (24)$$

$$V[Z_{0,0}] = MR \sum_{l=1}^{L} \alpha_l^2 \; E\left[\left(x_{g0}^n\right)^2\right]\frac{N_0}{2} + \frac{1}{MN} M^2 NR \sum_{l=1}^{L} \alpha_l^2 \; E\left[(x_{g0}^n)^2\right]\frac{N_0}{2} + MR\frac{N_0}{2}\frac{N_0}{2} \quad (25)$$

where E[.] and V[.] are the expectation and variance respectively. Also, the mean value, $E\left[(x_{g0}^n)^2\right]$ can be expressed in terms of the energy per bit, E_b as

$$E\left[(x_{g0}^n)^2\right] = \frac{MNE_b}{(M+N)R} \quad (26)$$

Therefore, Equations (24) and (25) in terms of E_b can be expressed as

$$E\left[Z_{0,0}\right] = \frac{NM^2E_b}{\sqrt{MN}(M+N)} \sum_{l=1}^{L} \alpha_l^2 \quad (27)$$

$$BER = \frac{1}{2}\text{erfc}\left(\frac{2(M+N)}{M \sum_{l=1}^{L} \alpha_l^2} \frac{N_0}{E_b} + \frac{R(M+N)^2}{2NM^2 \left(\sum_{l=1}^{L} \alpha_l^2\right)^2}\left(\frac{N_0}{E_b}\right)^2\right)^{-\frac{1}{2}} \quad (30)$$

Defining $\gamma_b = \sum_{l=1}^{L} \alpha_l^2 \; E_b/N_0$, the BER of OMCS-DCSK becomes

$$BER = \frac{1}{2}\text{erfc}\left(\frac{2(M+N)}{M\gamma_b} + \frac{R(M+N)^2}{2NM^2 {\gamma_b}^2}\right)^{-\frac{1}{2}} \quad (31)$$

Defining $\overline{\gamma_l} = E[\alpha_l^2]\, E_b/N_0$, the probability density function of γ_b was reported in [17], and given by

$$f(\gamma_b) = \frac{1}{\overline{\gamma_l}^L (L-1)!} \; e^{\frac{\gamma_b}{\overline{\gamma_l}}} \quad (32)$$

Finally, the overall BER expression for OMCS-DCSK system over multipath Rayleigh fading channel is calculated by averaging the conditional BER formula in (31) over γ_b , as

$$BER_{OMCS\_DCSK} = \int_0^{+\infty} BER(\gamma_b) \times f(\gamma_b) d\gamma_b \quad (33)$$

Equation (31) is also valid for AWGN case, only the function γ_b is changed to $\gamma_b = E_b/N_0$ by substituting $\alpha_1 = 1 \; and \; \alpha_{l\neq 1} = 0$ then the conditional BER of OMCS-DCSK over AWGN is expressed as

$$V[Z_{0,0}] = \frac{2\,NM^2}{(M+N)} \sum_{l=1}^{L} \alpha_l^2 \; E_b \frac{N_0}{2} + MR\frac{N_0^2}{4} \quad (28)$$

According to [27], $Z_{0,0}$ can be represented as

Gaussian random variables and therefore, the BER analytic of the OMCS-DCSK system can be expressed in terms of the complementary error function (*erfc*) as

$$BER = \frac{1}{2}\text{erfc}\left(\frac{E[Z_{0,0}]}{\sqrt{2\,V[Z_{0,0}]}}\right) \quad (29)$$

Substituting (27) and (28) into (29) and rearranged them to get

$$BER_{AWGN} = \frac{1}{2}\text{erfc}\left(\frac{2(M+N)}{M} \frac{N_0}{E_b} + \frac{R(M+N)^2}{2NM^2}\left(\frac{N_0}{E_b}\right)^2\right)^{-\frac{1}{2}} \quad (34)$$

3.3. Spectral and Rate Analysis

In this subsection, the percentage factors of bandwidth efficiency, energy saving and information rate are derived. The percentage form of bandwidth efficiency (BE) of MCS-

DCSK, OCVSK, and OMCS-DCSK respectively are expressed as

$$BE_{\text{MCS-DCSK}} = \frac{M-2}{M\beta} \times 100\% \quad (35)$$

$$BE_{\text{OCVSK}} = \frac{M}{(M+1)\beta} \times 100\% \quad (36)$$

$$BE_{\text{OMCS-DCSK}} = \frac{MN}{(M+N)R} \times 100\% \quad (37)$$

where $BE_{\text{MCS-DCSK}}$, BE_{OCVSK} and $BE_{\text{OMCS-DCSK}}$ are the percentage form of BE of MCS-DCSk, OCVSK, and OMCS-DCSK systems respectively.

Defining $E_{b,MCS\_DCSK} = T_c \frac{M(M-1)\beta E[x_n^2]}{M-2}$, $T_{b,OCVSK} = T_c \frac{(M+1)\beta E[x_n^2]}{M}$ and

$$E_{b,OMCS\_DCSK} = T_c \frac{(M+N)RE[x_n^2]}{MN}$$

as MCS-DCSK, OCVSK, and OMCS-DCSK transmitted energy per bit respectively, where $E[x_n^2]$ is the mean square value of chaotic sequence x_n. Then, the percentage form of energy saving enhancement factor (*ESE*) of OMCS-DCSK compared with MCS-DCSK and OCVSK respectively are written as

$$ESE_1 = \left(1 - \frac{E_{b,OMCS-DCSK}}{TE_{b,MCS-DCSK}}\right) \times 100\%$$
$$= \left(1 - \frac{(M-2)(M+N)}{M^2N(M-1)}\right) \times 100\% \quad (38)$$

$$ESE_2 = \left(1 - \frac{E_{b,OMCS-DCSK}}{E_{b,OCVSK}}\right) \times 100\%$$
$$= \left(1 - \frac{(M+N)}{M(N+1)}\right) \times 100\% \quad (39)$$

Defining $T_{b,MCS-DCSK} = \frac{M\beta}{M-2}T_c$, $T_{b,OCVSK} = \frac{(M+1)\beta}{M}T_c$ end $T_{b,OMCS-DCSK} = \frac{(M+N)R}{MN}T_c$. Then, the percentage form of the information rate enhancement factor (IRE) of OMCS-DCSK compared with MCS-DCSK and OCVSK respectively are written as

$$IRE_1 = \left(\frac{T_{b,MC-DCSK}}{T_{b,OMCS-DCSK}} - 1\right) \times 100\% =$$
$$\left(\frac{NM^2}{(M-2)(M+N)} - 1\right) \times 100\%$$
(٤٠)

$$IRE_2 = \left(\frac{T_{b,OCVSK}}{T_{b,OMCS-DCSK}} - 1\right) \times 100\% =$$
$$\left(\frac{(N+1)M}{(M+N)} - 1\right) \times 100\%$$
(٤١)

Figs. (8-10) show the percentage form of *BE*, *IRE*, and *ESE* of OMCS-DCSK respectively compared with MCS-DCSK versus *M* and for *N* =4, 8, 16 and 32. It can be seen that increasing *N* will improve BE, ESE, and IRE of the proposed system compared with MCS-DCSK system. For instance, when *M*=60, $BE_{\mathrm{OMCS-DCSK}}$=2%, 3.75%, 7%, 12.65%, IRE_1 =100%, 288%, 630% and 1207% and ESE_1=99.15%, 99.57%, 99.77% and 99.87% for *N*=2, 4, 8 and 16 respectively.

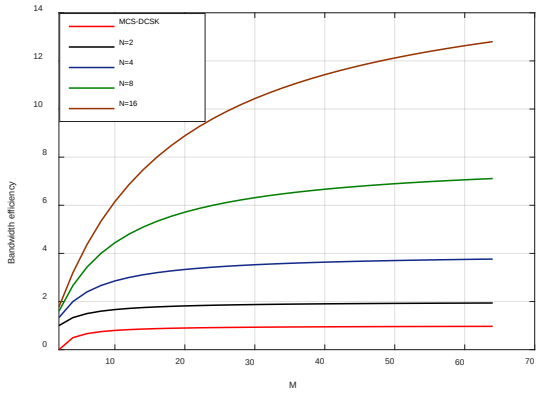

Figure8. *BE* comparisons between MCS-DCSK and the proposed system versus *M* values and *N*=2, 4, 8, and16.

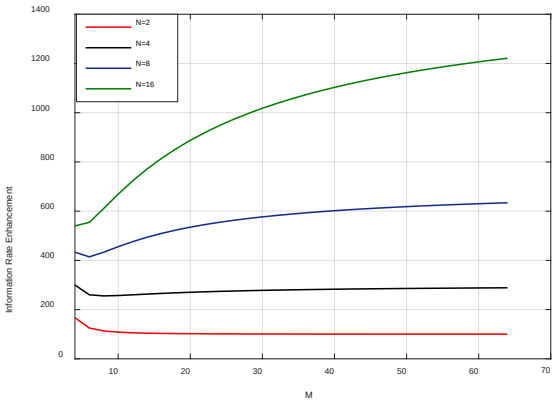

Figure 9. *IRE* comparisons between MCS-DCSK and the proposed system versus *M* values and *N*=2, 4, 8, and16.

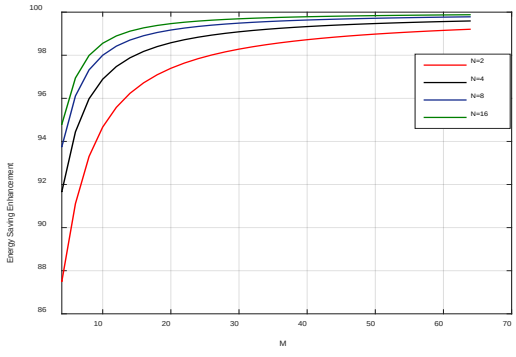

Figure 10. *ESE* of the proposed system comparing with MCS-DCSK versus *M* values and *N*=2, 4, 8, and16.

Figs. (11-13) show the percentage form of *BE*, *IRE*, and *ESE* of OMCS-DCSK respectively compared with OCVSK versus *N* and *M* =4, 8, 16 and 32. It can be seen that increasing *M* will improve *BE*, *ESE*, and *IRE* of the proposed system compared with OCVSK system. For instance, when *N*=60, $BE_{\mathrm{OMCS-DCSK}}$=2%, 3.75%, 7%, 12.65%, IRE_2 =96.75%, 280%, 617% and 1, 184% and ESE_2=49.2%, 73.7%, 86.1% and 92.2% for M=2, 4, 8 and 16 respectively.

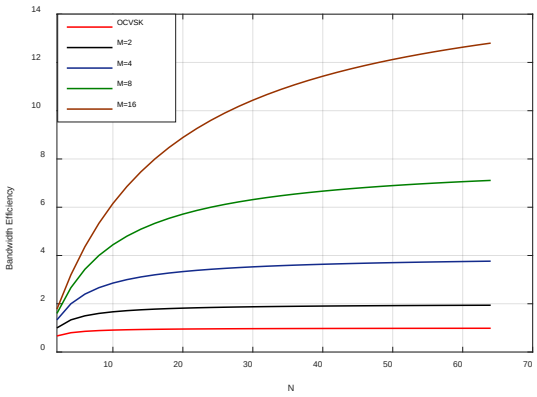

Figure11. *BE* of OMCS-DCSK comparing with OCVSK versus *N* and *M*=2, 4, 8 and 16.

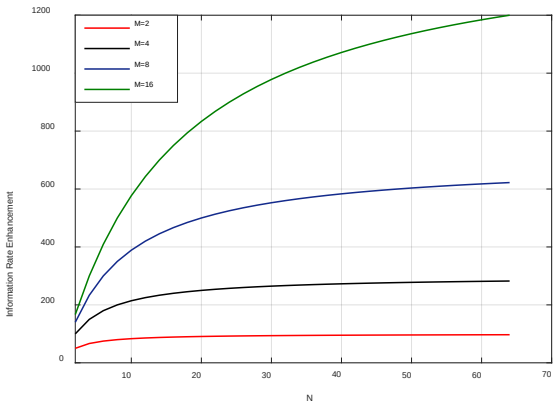

Figure 12. *IRE* of OMCS-DCSK comparing with OCVSK versus *N* and *M*=2, 4, 8, and 16.

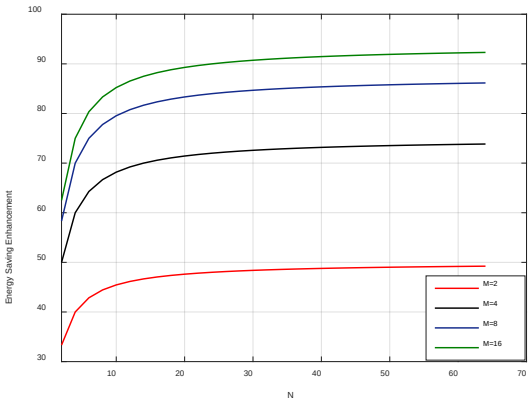

Figure 13. *ESE* of OMCS-DCSK comparing with OCVSK versus *N* and *M*=2, 4, 8, and 16.

3.4. Comparisons of Complexity

In this subsection, the comparison of the complexity between OMCS-DCSK and other systems such as MCS-DCSK and OCVSK is presented taking into consideration $\beta=R$ in all comparisons. The total complexity of the OMCS-DCSK system at transmitter and receiver to transmit *MN* bits can be expressed in terms of a number of additions (ADD_T), multiplications (MUL_T), divisions (DIV_T) and delay lines (DEL) as the following:

$$\begin{aligned} MUL_T &= 3M^2NR + MNR + MUL_{GS} \\ ADD_T &= (MN-1)MR + MN(MR-1) + ADD_{GS} \\ DIV_T &= DIV_{GS} \\ DEL &= 2MN \end{aligned} \quad (42)$$

where $MUL_{GS}=(R-1)(M^2+M-1)$, $ADD_{GS}=RM^2$, and $DIV_{GS}=RM$ are the multiplication, addition and division operations of the Gram-Schmidt process that are calculated according to [19]. Table 1 shows the complexity comparison in terms of MUL, ADD, and DEL and the Gram-Schmidt (GS) to ADD and MUL in the transmitter and receiver side. From this table, it can be seen that the complexity of OMCS-DCSK system is more than complexity of MCS-DCSK and OCVSK systems. However, the transmitted bits in MCS-DCSK and OCVSK are less than in OMCS-DCSK and the proposed system has better BER and higher data rate.

Table 1. Complexity comparisons of MCS-DCSK, OCV-DCSK and OMCS-DCSK systems

M	N	Bit send	System	Number Of DEL	Num-ber of ADD	Number of MUL	GS ADD	GS MUL	GS DIV
4	-	2	MCS_DCSK [9]	6	19β -2	26β -8	-	-	-
-	4	4	OCV-DCSK[29]	8	6β	8β	19(β-1)	16β	4β
4	1	4	OMCS_DCSK	8	28R-4	52R	(R-1)	R	R
8	-	6	MCS_DCSK [9]	14	103β -6	118β -48	-	-	-
-	8	8	OCV-DCSK[29]	16	14β	16β	71(β-1)	64β	8β
8	1	8	OMCS_DCSK	16	120R -8	200R	(R-1)	R	R
16	1	14	MCS_DCSK [9]	30	463β -14	494β -224	-	-	-
-	16	16	OCV-DCSK [29]	32	30β	32β	271 (β-1)	256β	16β
16	1	16	OMCS_DCSK	32	496R -16	784R	(R-1)	R	R

4. Simulation Results and Discussions

In this section, the performance of the OMCS-DCSK system over AWGN and multipath fading channel are evaluated and compared with BER analytically derived in section III. Also, the results will be compared with DCSK, QCSK, OCVSK and MC-DCSK systems. The parameters settings in these simulations are included: *N*, *M*=2, 4, 8, 16 and 32. Two paths Rayleigh fading channel, *L*=2, will be used with delays, $\tau_1 = 0$ and $\tau_2 = 2T_c$ and average power gain, $E[\alpha_1^2] = 2/3$ and $E[\alpha_2^2] = \frac{1}{3}$ [10].

4.1 Performance Evaluation

Fig. 14 shows the performance comparison between the simulated and analytic BER of OMCS-DCSK with *N*=4, *R*=100 and different *M* under various SNR over AWGN channel. Fig. 15 shows the performance comparison between the simulated and BER analytic of OMCS-DCSK with *M*=4, *R*=100 and different *N* under various SNR over AWGN channel. It can be observed that the simulated results agree with the analytic BER results, which confirms the theoretical analysis. Also, increasing the value of *M* will enhance BER performance and bit rate respectively, while increasing *N* values will degrade BER performance this is due to increase the length of information chaotic sequence and hence increase the noise interference. Fig. 16 shows the BER performance of OMCS-DCSK over AWGN with *R*=100 and in cases *M*=*N*, *M*<*N* and *M* >*N* conditions. When *M* >*N* (*M*=8 and *N*=2), the best BER performance is obtained. Fig. 17 shows the BER performance of OMCS-DCSK in AWGN channel for *M*=*N*=8 and *R* =50,100 and 200. It is clear that increasing R will decrease the performance for the same reason when N is increased, where any increased in R by a factor of two (50, 100, 200) leads to reduce the gained SNR by 0.8 dB in each case. Likewise here, the results approximately match for both analytic and the simulation cases. The same scenario is applied for multipath Rayleigh fading channel and the same observation results are obtained as shown in Figs. (18-20) respectively.

.

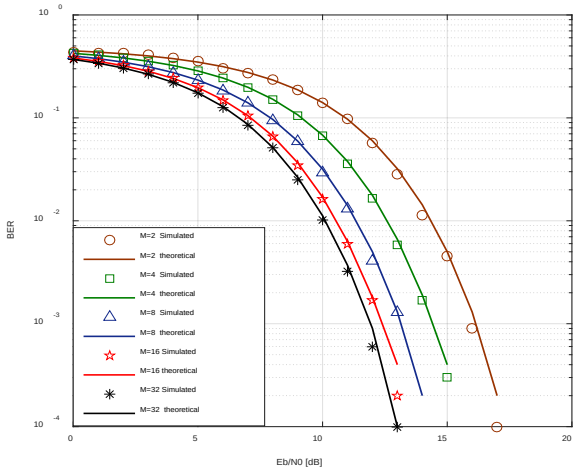

Figure14. Comparison between analytic BER and simulated performance of OMCS-DCSK system over AWGN channel with *R*=100, *N*=4 for different *M*.

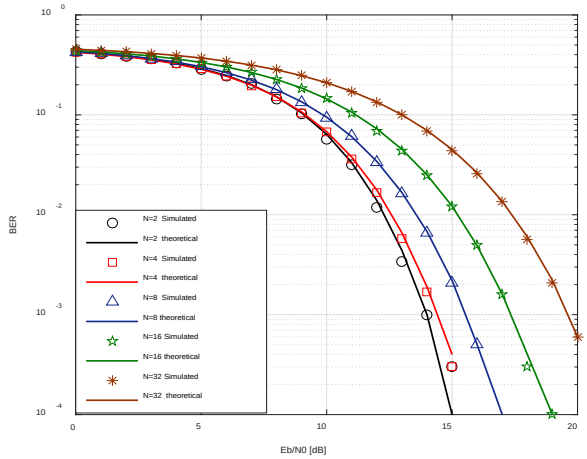

Figure 15. Comparison between analytic BER and simulated performance of OMCS-DCSK system over AWGN channel with *R*=100, *M*=4 for different *N*.

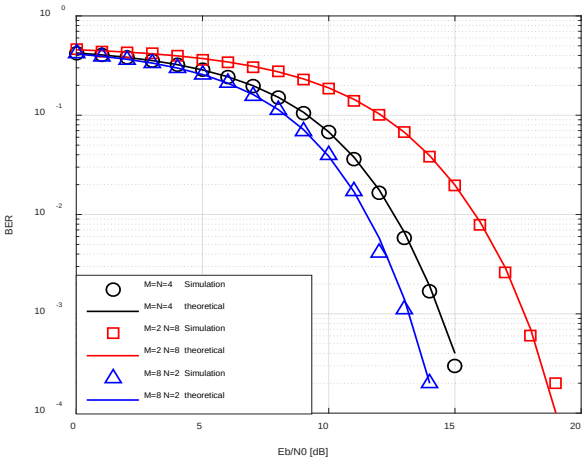

Figure16. BER performance of OMCS-DCSK system over AWGN channel with *R*=100, *M*=*N*, *M*<*N* and *M*>*N*.

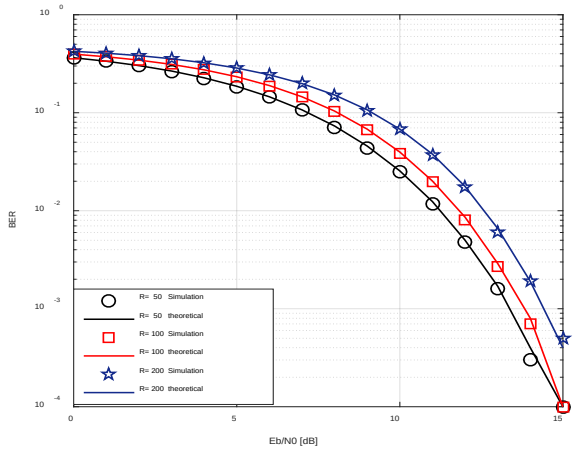

Figure17. BER performance of OMCS-DCSK system over AWGN channel with *M*=*N*, and *R*=50,100 and 200.

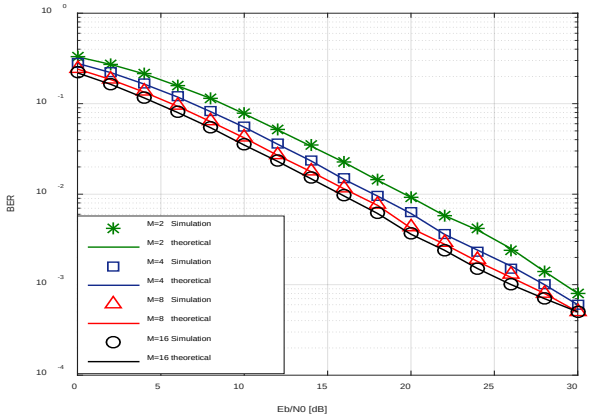

Figure 18. Comparison between analytic BER and simulated performance of OMCS-DCSK system over two paths Rayleigh fading channel with *R*=100, *N*=4 for different *M*.

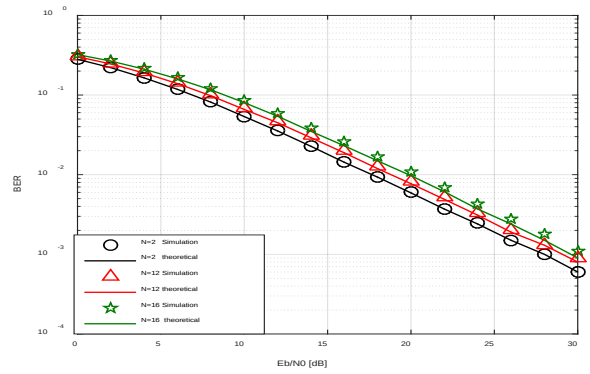

Figure 19. Comparison between analytic BER and simulated performance of OMCS-DCSK system over two paths Rayleigh fading channel with *R*=100, *M*=4 and different *N*.

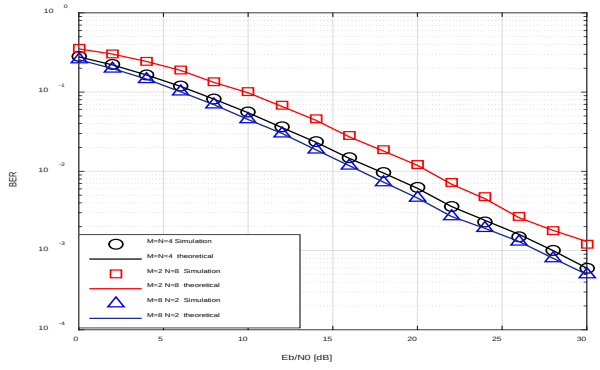

Figure 20. BER performance of OMCS-DCSK system over two paths Rayleigh fading channel with *R*=100, *M*=*N*, *M*<*N* and *M*>*N*.

4.2 Comparisons with Conventional Systems

Figs. 22 and 23 show the performance comparison of OMCS-DCSK system with the conventional DCSK systems including DCSK, QCSK, OCVSK and MCS-DCSK systems over AWGN with β=R=100 and two-paths Rayleigh fading channel with β=R=40 respectively and the transmitted bits number carries 128 bits in each frame, where β is the spreading factor length in DCSK,QCSK, OCVSK and MCS-DCSK systems. The OMCS-DCSK system has M=32 and N=4 and carries 128 bits in each frame while MCS-DCSK and OCVSK carry 126 and 4 bits respectively. It can be observed that over AWGN at BER = 10^{-3}, the SNR gain of the proposed system against DCSK, QCSK, OCVSK, MCS-DCSK are 4.4 , 3.4, 6.2 and 1 dB respectively . Also, the SNR gain of the proposed system at BER = 10^{-3} over two-path Rayleigh fading channel against DCSK, QCSK and MCS-DCSK are 5, 3 and 2 dB respectively. Therefore, the proposed OMCS-DCSK system has superior performance over other conventional systems regarding capability of transmitted bit number and BER.

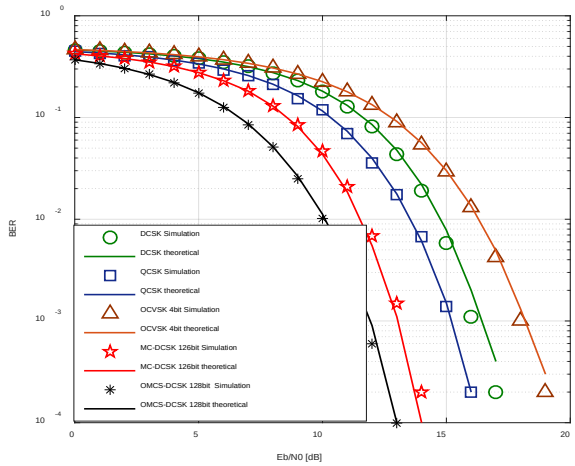

Figure 22. BER performance comparisons of OMCS-DCSK with other conventional systems over AWGN channel with β = R=100

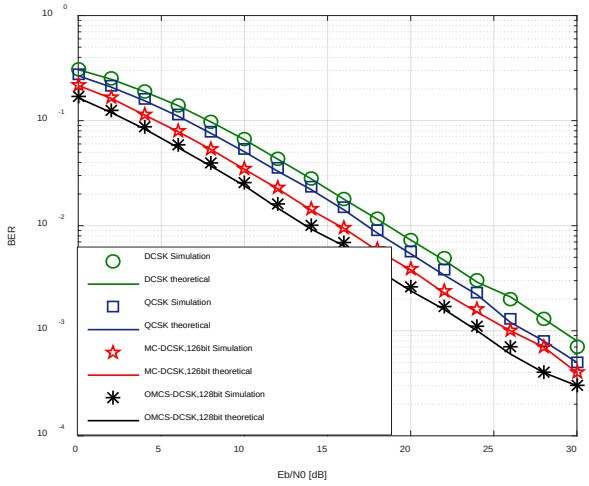

Figure23. BER performance comparisons of OMCS-DCSK with other conventional systems over two paths Rayleigh fading channel with β = R=40

5. Conclusions

In this paper, a new high data rate DCSK communication system is designed, analyzed and evaluated, in which new orthonormal basis signals are generated using Gram-Schmidt algorithm as in OCVSK system and Walsh code function as in MCS-DCSK system. It high data bits can be transmitted at the same time slot. In these systems, we need to transmit the N chaotic reference signals to detect the transmitted bits differentially. The bandwidth efficiency, energy saving enhancement, information rate enhancement factor and analytic BER of the proposed system are derived. The simulation results show that the proposed system has superior results in *BE*, *ESE* and *IRE* compared with conventional DCSK system. Also, the matching of BER simulation to analytical BER is clearly noticed in the figures. In addition, the performance dependency of the proposed system on the number of Gram-Schmidt, N, Walsh code length, M, and spreading factor, R, is studied. Finally, the performance comparison with other conventional systems, including DCSK, QCSK, OCVSK, and MCS-DCSK are presented.

Acknowledgements

This work is supported by Electrical Department/ Faculty of Engineering/ Mustansiriyah University.

Conflict of interest

There are not conflicts to declare.

4. References

1. A. Abel and W. Schwarz, (2002) *"Chaos communications-principles, schemes, system analysis, " Proc. IEEE*, vol. 90, pp. 691–710, May.
2. F. C. M. Lau and C. K. Tse, (2003) *"Chaos-Based Digital Communication Systems," New York: Springer-Verlag*.
3. G. Kolumbán, G. Kis, Z. Jákó, and M. P. Kennedy, (1998) *"FM-DCSK: A robust modulation scheme for chaotic communications," IEICE Trans. Fundam. Electron. Commun. Comput. Sci.*, vol. E81-A, no. 9, pp. 1798–1802, Oct.
4. G. Kolumban, B. Vizvari, W. Schwarz, and A. Abel, (1996) *"Differential chaos shift keying: A robust coding for chaos communications," In Proc. Int. Workshop Nonlinear Dyn. Electron. Syst., Seville, Spain*, pp. 87-92, Jun.
5. Z. Galias and G. M. Maggio, (2001) "*Quadrature chaos-shift keying: Theory and performance analysis," IEEE Trans. Circuits Syst.-I*, vol. 48, no. 12, pp. 1510-1519, Dec.
6. T.J. Wren T.C. Yang,(2010) *"Orthogonal chaotic vector shift keying in digital communications," IET Communications*, vol. 4, no. 6, pp. 739-753.
7. Wang L., Cai G. and Chen G.,(2015) *"Design and performance analysis of a new multiresolution M-ary differential chaos shift keying communication system", IEEE Transaction on Wireless Communications*, vol. 14, no.9,pp. 5197-5208.
8. W. Xu and L. Wang, (2011) *"A novel differential chaos shift keying modulation scheme," Int. J. Bifurcation Chaos*, vol. 21, no. 3, pp. 799–814.
9. Huang T., L. Wang, Xu W. and Lau F. C.**,** **(**2016**)** *"Multilevel code-shifted differential-chaos-shift-keying system," IET Communications*, vol. 10, no. 10, pp. 1189 – 1195,.
10. H. Yang, W. K. Tang, G. Chen, and G.-P. Jiang, (2016) *"System design and performance analysis of orthogonal multi-level differential chaos shift keying modulation scheme," IEEE Trans. Circuits Syst.-I*, vol. 63, no.1, pp. 146-156, Jan.
11. Hua Yang, Guo-Ping Jiang, and Junyi Duan,(2014) *"Phase separated DCSK: A simple delay-component-free solution for chaotic communications," IEEE Transactions on Circuits and Systems II: Express Briefs*, vol .61, no. 12, pp. 967 – 971, September.
12. G. Kaddoum, E. Soujeri, Carlos Arcila , and K. Eshteiwi, (2015) *" I-DCSK: an improved non-coherent communication system architecture," IEEE Transactions on Circuits and Systems II: Express Briefs*, vol. 62 , pp. 901 – 905, May.
13. G. Kaddoum, E. Soujeri, and Y. Nijsure, (2016) *"Design of a short reference non-coherent chaos-based communication systems," IEEE Transactions on Communications*, vol. 64, no. 2, pp. 680 – 689, January 2.
14. E. Soujeri, G. Kaddoum and M. Herceg, (2018) *"Design of an initial condition-index chaos shift keying modulation," Electronics Letters*, vol. 54, no. 7, pp. 447 – 449, April.
15. Kaddoum G., Gagnon F., Richardson F. D., (2012) *"Design of a secure multi-carrier DCSK system," IEEE International symposium on wireless communication systems*, pp. 964-8.
16. Kaddoum G., Richardson F. D. and Gagnon F., (2013) *"Design and analysis of a multi-carrier differential chaos shift keying communication system," IEEE Transactions on Communications*, vol. 61, no.8, pp. 3281-91.

17. Li S, Zhao Y, Wu Z., (2015) *"Design and analysis of an OFDM-based differential chaos shift keying communication system," Journal of Communications*, vol. 10, no. 3, pp. 199-205.
18. Fadhil S. Hasan, (2017) *"Design and analysis of an OFDM-based short reference quadrature chaos shift keying communication system," Wireless Personal Communications*, vol. 96, no. 2, pp. 2205–2222, September.
19. Fadhil S. Hasan, Alejandro A. Valenzuela, (2018) *"Design and Analysis of an OFDM-based Orthogonal Chaotic Vector Shift Keying Communication System," IEEE Access*, , vol. 6 , pp. 46322 - 46333, August.
20. E. Basar, M. Wen, R. Mesleh, M. Di Renzo, Y. Xiao and H. Haas, (2017) *"Index modulation techniques for next-generation wireless networks," IEEE Access*, vol. 5, pp. 16693-16746.
21. M. Herceg, D. Vranjes, G. Kaddoum and E. Soujeri, (2018) *"Permutation index DCSK modulation technique for secure multiuser high-data-rate communication systems," IEEE Trans. Veh. Tech.*, vol. 67, no. 4, pp. 2997-3011, April.
22. G. Kaddoum, M. F. A. Ahmed and Y. Nijsure, (2015) *"Code index modulation: A high data rate and energy efficient communication system," IEEE Commun. Lett.*, vol. 19, no. 2, pp. 175-178, Feb.
23. G. Kaddoum, Y. Nijsure and H. Tran, (2016) *"Generalized code index modulation technique for high-data-rate communication systems," IEEE Trans. Veh. Tech.*, vol. 65, no. 9, pp. 7000-7009, Sept.
24. M. Herceg, D. Vranjeˇs, G. Kaddoum and E. Soujeri, (2018) "Commutation cod index DCSK modulation technique for high-data-rate communication systems," *IEEE Trans. Circuits Syst. II, Exp. Briefs*., vol. 65, no. 12, pp.1954-1958, Dec.
25. W. Xu, T. Huang and L. Wang, (2017) "Code-shifted differential chaos shift *keying with code index modulation for high data rate transmission," IEEE Trans. Commun.*, vol. 65, no. 10, pp. 4285-4294, Oct.
26. X. Cai, W. Xu, D. Wang, S. Hong, L. Wang, (2019) *"An M-ary Orthogonal Multilevel Differential Chaos Shift Keying System with Code Index Modulation," IEEE Trans. Commun.*, vol. 67 , no. 7, pp. 4835 - 4847, July.
27. Y. Xia, C. K. Tse, and F. C. M. Lau, (2004) *"Performance of differential chaos shift-keying digital communication systems over a multipath fading channel with delay spread," IEEE Trans. Circuits and Systems II*, vol. 51, pp. 680–684,.
28. G. Kaddoum, E. Soujeri,(2016) *"NR-DCSK: A noise reduction differential chaos shift keying system", IEEE Trans. Circuits Syst. II Exp. Briefs*.
29. Fadhil S. Hasan, (2017) *"Design and Analysis of an Orthogonal Chaotic Vectors based Differential Chaos Shift Keying Communication System,"* Al-Nahrain Journal for Engineering Sciences (NJES), vol.20 No.4, pp.952-958.